argon-bubbled CH_3CN acquired at various times after excitation with a 420-nm, 6-ns laser pulse (≤5.2 mJ/pulse) are shown in Figure 1. The spectra are corrected for emission. At 20 ns after the excitation pulse, increased absorbance at 370 nm due to the bipyridyl anion radical and bleaching at 440–460 nm due to the loss of the ground-state, $d\pi(Ru^{II}) \rightarrow \pi^*(b,m)$ transition were observed, in addition to absorptions in the 490–690-nm region. At later times, the 370-nm absorption shifted to 390 nm, the bleaching disappeared, and absorptions in the visible region increased in intensity with maxima at 510 and 610 nm. The band at 510 nm is due to $PTZpn^{\bullet+}$,[11] while the bands at 390 and 610 nm are due to $prPQ^{\bullet+}$.[12] By 45 ns after the pulse, the difference spectrum corresponded to a superposition of the spectra of $PTZpn^{\bullet+}$ and $prPQ^{\bullet+}$, consistent with the formation of the redox-separated state, $[(PTZpn^{\bullet+})\text{-}Lys(Ru^{II}b_2m)^{2+}\text{-}NH\text{-}(prPQ^{\bullet+})]$. The maximum absorbance increase at 610 nm occurred 45 ns after the excitation pulse, after which the difference spectrum decayed monoexponentially to the base line with a lifetime of 146 ± 3 ns ($k_7 = 6.9 \pm 0.2 \times 10^6\ s^{-1}$). The observed monoexponential decay implies that a single conformation of the triad predominates in solution or, more likely, that the conformational equilibria which exist for the interconversion between conformers are rapid on the time scale of the electron transfer. The energy stored in the redox-separated state was 1.14 V, based on the measured redox potentials of the donor and acceptor of the triad.

Analysis of transient absorption and emission data for the model dyads allows us to assign values to some of the rate constants in Scheme I. The rate constant for the appearance of $PTZpn^{\bullet+}$ in the triad, $k_1 = 1.3 \times 10^8\ s^{-1}$, was the same within experimental error as that obtained for quenching of the MLCT excited state in the dyad $[PTZpn\text{-}Lys(Ru^{II}b_2m)^{2+}\text{-}OCH_3]$, based on analysis of rise-time kinetics monitored at 510 nm. The appearance of $prPQ^{\bullet+}$ in the triad occurs with a rate constant indistinguishable from that for the appearance of $PTZpn^{\bullet+}$. This is more rapid than MLCT quenching in the dyad $[Boc\text{-}Lys(Ru^{II}b_2m)^{2+}\text{-}NH\text{-}prPQ^{2+}]$, $k = 3 \times 10^7\ s^{-1}$. From the ratio of rate constants for the models it can be inferred that $k_4/k_1 \sim 0.2$, indicating that the left-hand branch makes a relatively small contribution to excited-state quenching. We conclude that the redox-separated state is formed primarily via the k_1 step followed by k_2, with k_2 rapid on the time scale of the spectroscopic experiment, $\geq 2 \times 10^8\ s^{-1}$. There was no evidence for $prPQ^{\bullet+}$ in transient absorption difference spectra of $[Boc\text{-}Lys(Ru^{II}b_2m)^{2+}\text{-}prPQ^{2+}]$, even though the MLCT emission was efficiently quenched, from which it can be inferred that $k_6 \gg k_4$ in Scheme I.[13] The redox-separated state of the PTZ dyad, $[(PTZpn^{\bullet+})\text{-}Lys(Ru^{II}b_2m)^{2+}\text{-}OCH_3]$, was observed and exhibited a lifetime of $\tau = 25$ ns ($k_3 = 4 \times 10^7\ s^{-1}$) following laser-flash photolysis. Note that the addition of a second electron-transfer step in the triad resulted in a 6-fold increase in the redox-separated state lifetime.

At its maximum appearance, the redox-separated state of the triad was formed with a quantum yield, Φ_{rss}, of 0.34 ± 0.03. This value was measured relative to the efficiency of formation of $PQ^{\bullet+}$ following oxidative quenching of $(Ru^{II}b_3)^{2+}$ by PQ^{2+}.[14] The less-than-unit efficiency in the formation of the redox-separated state must originate in the deactivational processes, k_3 and/or k_6 in Scheme I. From the high degree of emission quenching, the initial electron transfer is rapid and efficient. Neglecting the left-hand branch of Scheme I, using the values for k_1, k_3, and k_4 obtained from the model dyads, and $\Phi_{rss} = 0.34$, we calculate $k_2 \sim 2.9 \times 10^7\ s^{-1}$ ($\tau = 35$ ns). This is not consistent with the experimental observation that $prPQ^{\bullet+}$ appears with $k \sim 1.3 \times 10^8\ s^{-1}$. There may be a significant contribution from the left-hand branch of the mechanism in Scheme I or a change in rate constants in the triad compared to the model dyads.

It is possible to convert the stored energy of the redox-separated state into chemical redox energy.[15] Formation of the redox-separated state of the triad in freeze–pump–thaw–degassed CH_3CN with 532-nm excitation in the presence of both 4 mM tetramethylbenzidine (TMBD) and 3 mM benzoquinone (BQ) was followed by electron transfer from TMBD to $PTZpn^{\bullet+}$ ($k = 6 \times 10^9\ M^{-1}\ s^{-1}$) and electron transfer from $prPQ^{\bullet+}$ to BQ ($k = 1 \times 10^9\ M^{-1}\ s^{-1}$). The electron-transfer reactions, which followed pseudo-first-order kinetics, were observed by monitoring the quenching of the transient absorption of $PTZpn^{\bullet+}$ by TMBD and the quenching of $prPQ^{\bullet+}$ by BQ. In the net reaction visible light was converted into the chemical redox energy of the transient products, $TMBD^{\bullet+}$ and $BQ^{\bullet-}$.[16-17]

$$TMBD + BQ \xrightarrow[\text{lysine triad}]{h\nu_{532nm}} TMBD^{\bullet+} + BQ^{\bullet-} \quad \Delta G^\circ = 0.8\ eV$$

Using redox modules such as those described here, we are pursuing the assembly of more complex redox-active peptides.

Acknowledgment is made to the National Science Foundation (Grant CHE-8806664), the National Institute of General Medical Sciences (Grants GM32296 and GM42031), and the North Carolina Biotechnology Center (Grant 8913-ARIG-0104) for support of this research.

Supplementary Material Available: Characterization data for the compounds synthesized (3 pages). Ordering information is given on any current masthead page.

(11) Alkaitis, S. A.; Beck, G.; Grätzel, M. *J. Am. Chem. Soc.* **1975**, *97*, 5723.
(12) Watanabe, T.; Honda, K. *J. Phys. Chem.* **1982**, *86*, 2617.
(13) In order to establish that direct electron transfer between PTZpn and $prPQ^{2+}$ did not play a role, the dyad $[PTZpn\text{-}NH\text{-}prPQ^{2+}]$ was prepared.[9] This dyad showed no ground-state absorption above 375 nm. In contrast, a concentrated solution of 10-MePTZ and PQ^{2+} showed a charge-transfer absorption for the 10-MePTZ,PQ^{2+} donor–acceptor complex at 500 nm.
(14) Olmsted, J., III; Meyer, T. J. *J. Phys. Chem.* **1987**, *91*, 1649.
(15) (a) Young, R. C.; Meyer, T. J.; Whitten, D. G. *J. Am. Chem. Soc.* **1975**, *97*, 4781. (b) Nagle, J. K.; Bernstein, J. S.; Young, R. C.; Meyer, T. J. *Inorg. Chem.* **1981**, *20*, 1760.
(16) Takemoto, K.; Matsusaka, H.; Nakayama, S.; Suzuki, K.; Ooshika, Y. *Bull. Chem. Soc. Jpn.* **1968**, *41*, 764.
(17) (a) Foster, R.; Thompson, T. J. *Trans. Faraday Soc.* **1962**, *58*, 860. (b) Slifkin, M. A. *Spectrochim. Acta* **1964**, *20*, 1543.

NMR Assignment Strategy for DNA Protons through Three-Dimensional Proton–Proton Connectivities. Application to an Intramolecular DNA Triplex

Ishwar Radhakrishnan and Dinshaw Patel

Department of Biochemistry & Molecular Biophysics
Columbia University
630 West 168th Street, New York, New York 10032

Xiaolian Gao*

Department of Structural & Biophysical Chemistry
Glaxo Research Institute
Research Triangle Park, North Carolina 27709

Received July 11, 1991

Homonuclear three-dimensional (3D) proton NMR has been shown to be useful in both resonance assignments and structure determination of proteins and saccharides.[1-7] This technique is

(1) Griesinger, C.; Sørensen, O. W.; Ernst, R. R. *J. Am. Chem. Soc.* **1987**, *109*, 7227–7228.
(2) (a) Vuister, G. W.; Boelens, R.; Kaptein, R. *J. Magn. Reson.* **1988**, *80*, 176–185. (b) Vuister, G. W.; de Waard, P.; Boelens, R.; Vliegenthart, J. F. G.; Kaptein, R. *J. Am. Chem. Soc.* **1989**, *111*, 772–774. (c) Vuister, G. W.; Boelens, R.; Padilla, A.; Kleywegt, P. G.; Kaptein, R. *Biochemistry* **1990**, *29*, 1829–1839. (d) Padilla, A.; Vuister, G. W.; Boelens, R.; Kleywegt, G. J.; Cavé, A.; Parello, J.; Kaptein, R. *J. Am. Chem. Soc.* **1990**, *112*, 5024–5030. (e) Breg, J. N.; Vuister, G. W.; Kaptein, R. *J. Magn. Reson.* **1990**, *87*, 646–651.
(3) Oschkinat, H.; Cieslar, C.; Holak, T. A.; Clore, G. M.; Gronenborn, A. M. *J. Magn. Reson.* **1989**, *83*, 450–472.
(4) Oschkinat, H.; Cieslar, C.; Griesinger, C. *J. Magn. Reson.* **1990**, *86*, 453–469.
(5) Holak, T. A.; Habazettl, J.; Oschkinat, H.; Otlewski, J. *J. Am. Chem. Soc.* **1991**, *113*, 3196–3198.

0002-7863/91/1513-8542$02.50/0

Scheme I

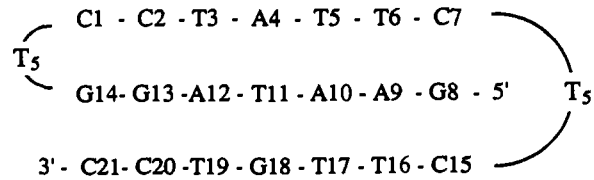

particularly needed when chemical and biochemical synthesis of uniformly isotope enriched material of large systems, such as oligonucleotide sequences, is not readily available. A 3D NOESY–TOCSY spectrum of a DNA dodecamer has recently been presented,[8] which demonstrated the separation of overlapped two-dimensional (2D) NOE cross peaks involving cytidine residues in the base and sugar proton region by using the H5–H6 scalar (J) coupling correlations in the 3D NMR spectrum. In this paper we present a general strategy for nearly complete proton assignments in a right-handed DNA sequence through the three-dimensional dipolar–scalar coupling connectivities observed in a 3D NOESY–TOCSY spectrum by using a 31-mer DNA triplex as an example.

The sequence and secondary folding of the triplex used in this work are shown in Scheme I. This triplex contains 21 residues, and each of the two loops contains five thymidines. In a NOESY–TOCSY spectrum, the $\omega1$–$\omega2$ correlations correspond to the NOE connectivity and the $\omega2$–$\omega3$ correlations correspond to the J connectivity. We have used spectral planes intersecting the $\omega3$ axis at the H1′ and Cyt(H5) frequency range to observe NOE cross peaks at positions $\omega1 \neq \omega2 \neq \omega3$. These cross peaks are observed through the J-coupling frequency filter, which permits the selective assignment of through-space sequential connectivities between consecutive nucleotide residues (vide infra). The reason that H1′ and Cyt(H5) resonances were chosen at the $\omega3$ dimension is two-fold: first, the efficiency of J–NOE magnetization transfer through H1′ and Cyt(H5) is high, and second, the H1′ protons are better resolved than other sugar protons, consequently offering better spectral simplification in the related $\omega1$–$\omega2$ planes.

In the following, we demonstrate a new approach, which differs from the conventional proton assignment methods utilizing 2D NOESY spectra, for the assignment of DNA protons through 3D connectivities. 2D proton assignments rely on sequential connectivities of the H8 or H6 base protons to the H1′ protons of the same and the preceding residues, since the base to H1′ proton spectral region is best resolved in a 2D NOESY spectrum.[9] Poor resolution of the base or H1′ protons prohibits detailed studies of moderate to large molecules (>30 residues), such as biologically interesting triplexes and quadruplexes. In a 3D NOESY–TOCSY spectrum, these H8 or H6 and H1′ cross peaks reside on the NOE lines ($\omega2 = \omega3$) at the planes viewed through the H1′ frequencies. These 3D cross peaks do not provide resolution enhancement as compared to their 2D counterparts. Instead, we observed, on the H1′ planes of the 3D spectrum, well-resolved NOE connectivities linking H2′,2″ protons of residue i with the H8 or H6 protons of residues i and $i + 1$ (Figure 1). Starting from the H1′ plane of residue i and proceeding to the next H1′ plane, which contains the $i + 1$ H8 or H6 resonance, the complete network of intra- and interresidue H2′,2″–H8 or H2′,2″–H6 connectivities along the sequence can be traced. For example, Figure 1a shows a plane at 6.05 ppm ($\omega3$ = A9(H1′)), which exhibits NOE cross peaks linking the H2′ and H2″ protons of A9 (note that only protons J-coupled to the A9(H1′) can be observed along the $\omega2$ axis) with the H8 protons of their own and the A10 residue. The plane at 6.02 ppm ($\omega3$ = A10(H1′)) in Figure 1b exhibits NOE cross peaks between H2′,2″ protons of A10 and the H8 proton of A10 as well as the H6 proton of T11. Similarly, on the plane at 5.89 ppm

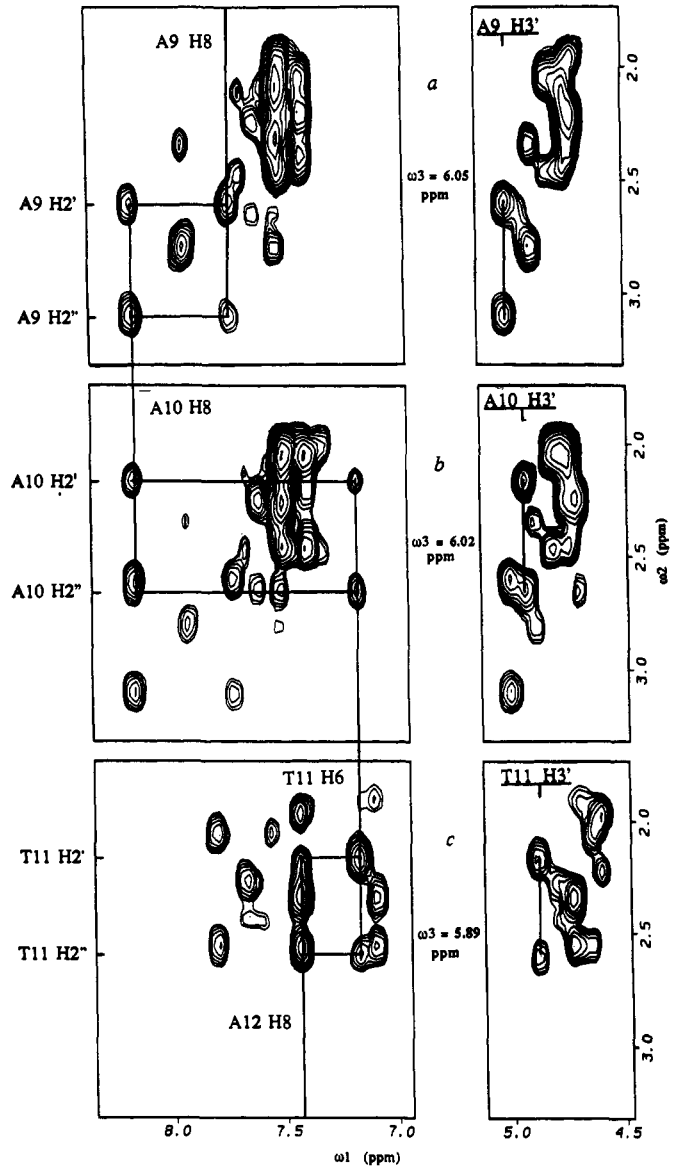

Figure 1. 3D NOESY–TOCSY spectrum[2a,7] of the DNA triplex recorded on a Bruker AMX500 spectrometer at 25 °C in D_2O solution containing 10 mM PO_4 and 0.1 mM EDTA, pH 4.9. The mixing times for NOE and spin-lock are 200 and 28 ms, respectively. The spectrum covers a spectral width of 4200 Hz (8.4 ppm) and contains 256 × 66 × 128 complex data points in $\omega3/\omega2/\omega1$ dimensions, respectively. Eight transients were accumulated for each FID. Data processing was carried out as described previously,[7] and final spectral size is 256 × 256 × 256 in real points. The expanded contour plots show NOE connectivities in the base ($\omega1$: 6.9–8.3 ppm) and H2′,2″ ($\omega2$: 1.7–3.2 ppm) region (left panel) as well as the H3′ ($\omega1$: 4.5–5.1 ppm) and H2′,2″ ($\omega2$: 1.7–3.2 ppm) region (right panel) through the frequencies of (a) $\omega3$ = 6.05 ppm (A9(H1′)), (b) $\omega3$ = 6.02 ppm (A10(H1′)), and (c) $\omega3$ = 5.89 ppm (T11(H1′)). These expanded spectra demonstrate the enhanced resolution in the H2′,2″ to aromatic proton region and sequential assignments for residues 9, 10, and 11 (plots on the left). The overlaps in the H2′,2″ to H3′ proton region of this 31-mer sequence are greatly reduced, such that the connectivities from H2′,2″ to H3′ protons can be identified and used for the assignment of sequential connectivities.

($\omega3$ = T11(H1′)), the connectivities from the H2′,2″ of T11 to the intraresidue H6 and interresidue A12(H8) were found (Figure 1c). Following this procedure, we were able to proceed from the 5′- to the 3′-end for each of the three strands in the triplex stem and assign all the base, H1′, H2′,2″, H3′ and some of the H4′ and H5′,5″ resonances.[10] Protons of the 10 individual thymidine

(6) Wijmenga, S. S.; van Mierlo, C. P. M. *Eur. J. Biochem.* **1991**, *195*, 807–822.
(7) Gao, X.; Burkhart, W. *Biochemistry* **1991**, *30*, 7730–7739.
(8) Piotto, M. E.; Gorenstein, D. G. *J. Am. Chem. Soc.* **1991**, *113*, 1438–1440.
(9) Wüthrich, K. *NMR of Proteins and Nucleic Acids*; John Wiley & Sons: New York, 1986 and reference cited therein.
(10) Radhakrishnan, I.; Gao, X.; Patel, D. J. "Proton Assignments of an Intramolecular DNA Triplex Containing a GTA triplet. Application of 2D and 3D NMR Spectroscopy", in preparation.

residues in the loops were also identified, although there is little interresidue contact in the loop structure to permit specific assignments. In this approach, the correct identification of the H2′,2″ geminal proton pair is critical. This can be easily achieved in our case, for the 31-mer DNA sequence, by observing well-resolved strong H2′–H2″[10] and moderate H3′–H2′ and H3′–H2″ cross peaks on the same spectral plane (right panel of Figure 1). A major complication in data analysis arises from the presence of the so-called "cross-talk" cross peaks[2c] due to the resolution limitation of the 3D data set (Figure 1a,b). These ambiguities can be removed in most cases by comparing the relative intensities of these cross peaks and the spectral patterns in adjacent planes.

The strategy to assign DNA resonances through 3D NOE–*J* connectivities shown herein uses H1′ planes along the ω3 dimension in the NOESY–TOCSY spectrum and H2′,2″ to base proton connectivities observed on these H1′ planes. The assignment is assisted by spectral regions of H2′–H2″ and H3′–H2′,2″ on the ω3 = H1′ planes. The NOE connectivities observed on the H1′ planes exhibit enhanced clarity and a characteristic correlation pattern. By contrast, the H2′,2″ to base proton NOE cross peaks of a large DNA molecule in a 2D data set are often too crowded to be of primary use, and the cross peaks in H2′–H2″ and H3′–H2′,2″ regions are extensively overlapped. The H5 planes of the cytidine residues provide well-resolved sequential connectivities of the H6 with the H2′,2″ protons for the intra- and interresidues,[8] permitting verification of the assignments made at the corresponding H1′ planes.[10] Other spectral regions are helpful in verifying the assignments. 3D proton–proton NMR spectroscopy presents great potential in the studies of increasingly larger DNA molecules as illustrated by its application to the proton assignment of this 31-mer DNA triplex.[10] The assignment strategy used in this work should be applicable to the interpretation of 3D TOCSY–NOESY data and could also be extended to the resonance assignments of ribonucleotide sequences.

Acknowledgment. This work was supported in part by NIH Grant GM34504 to D.P.

Spectroscopic Characterization of the Peroxide Intermediate in the Reduction of Dioxygen Catalyzed by the Multicopper Oxidases

James L. Cole,† David P. Ballou,‡ and Edward I. Solomon*,†

Department of Chemistry, Stanford University Stanford, California 94305
Department of Biological Chemistry The University of Michigan, Ann Arbor, Michigan 48109
Received June 14, 1991

The multicopper oxidases (laccase, ascorbate oxidase, and ceruloplasmin)[1] catalyze the four-electron reduction of dioxygen to water. These enzymes contain type 1 (blue), type 2 (normal), and type 3 (coupled binuclear) copper centers. We have previously demonstrated that N_3^- binds to laccase and ascorbate oxidase as a bridging ligand between the type 2 site and one of the type 3 coppers, thereby defining a novel trinuclear copper cluster.[2] A recent X-ray structure of ascorbate oxidase supports this cluster model.[3] The reduced trinuclear site in a type 1 Hg^{2+}-substituted

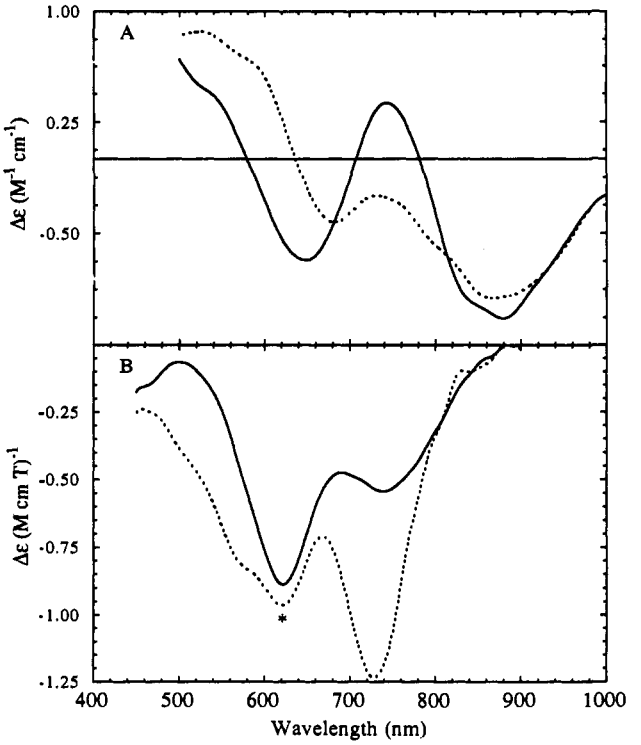

Figure 1. Ligand-field spectra of the T1Hg laccase intermediate. (A) Room temperature CD: (—), oxygen intermediate; (···), fully oxidized enzyme. [T1Hg] = 0.419 mM, [O_2] = 0.45 mM in 100 mM potassium phosphate, pH 7.4. The spectrum of the intermediate was recorded 1.5 min after oxygenation. At pH 7.4, $t_{1/2}$ for decay of the intermediate is ~1 h. Conditions: scan speed, 200 nm/min; time constant, 0.25 s. (B) MCD at 4.2 K and 7 T: (—), oxygen intermediate; (···), fully oxidized enzyme. [T1Hg] = 0.476 mM. The sample was reduced in 200 mM potassium phosphate, pH 7.4, and reoxidation was initiated by addition of an equal volume of O_2-saturated glycerol. The intermediate sample was frozen in liquid nitrogen after 3 min. The negative band at 614 nm (*) is associated with a ≤5% contaminant of native laccase.

laccase derivative (T1Hg) is reoxidized by dioxygen,[4] indicating that the trinuclear center represents the minimal structural unit capable of reducing dioxygen. In the course of these studies, we detected an intermediate in the reaction of T1Hg with dioxygen. Here we provide evidence that two electrons are transferred from the type 3 coppers to dioxygen, generating a peroxide intermediate. Stopped-flow data indicate that this species represents a precursor to the intermediate observed[5] upon reoxidation of native laccase. The absorption spectrum of the laccase peroxide intermediate is strikingly different from that of oxyhemocyanin, and it is suggested that the laccase intermediate contains a μ-1,1 hydroperoxide that bridges one of the oxidized type 3 coppers and the reduced type 2 copper.

For MCD and CD studies, T1Hg laccase[6] was reduced by anaerobic dialysis against 5 mM sodium dithionite in 100 mM

† Stanford University.
‡ The University of Michigan.

(1) (a) Malkin, R.; Malmström, B. G. *Adv. Enzymol.* **1970**, *33*, 177. (b) Malmström, B. G.; Andréasson, L.-E.; Reinhammar, B. In *The Enzymes*; Boyer, P. D., Ed.; Academic: New York, 1975; Vol. XII. (c) Fee, J. A. *Struct. Bonding (Berlin)* **1975**, *23*, 1–60. (d) Solomon, E. I. In *Copper Proteins*; Spiro, T. G., Ed.; Wiley-Interscience; New York, 1981; pp 41–108. (e) Solomon, E. I.; Penfield, K. W.; Wilcox, D. E. *Struct. Bonding (Berlin)* **1983**, *53*, 1.

(2) (a) Allendorf, M. D.; Spira, D. J.; Solomon, E. I. *Proc. Natl. Acad. Sci. U.S.A.* **1985**, *82*, 3063–3067. (b) Spira-Solomon, D. J.; Allendorf, M. D.; Solomon, E. I. *J. Am. Chem. Soc.* **1986**, *108*, 5318–5328. (c) Cole, J. L.; Clark, P. A.; Solomon, E. I. *J. Am. Chem. Soc.* **1990**, *112*, 9534–9548. (d) Cole, J. L.; Avigliano, L.; Morpurgo, L.; Solomon, E. I. *J. Am. Chem. Soc.*, in press.

(3) (a) Messerschmidt, A.; Rossi, A.; Ladenstein, R.; Huber, R.; Bolognesi, M.; Gatti, G.; Marchesini, A.; Petruzzelli, R.; Finazzi-Agrò, A. *J. Mol. Biol.* **1989**, *206*, 513–529. (b) Messerschmidt, A.; Huber, R. *Eur. J. Biochem.* **1990**, *187*, 341–352.

(4) Cole, J. L.; Tan, G. O.; Yang, E. K.; Hodgson, K. O.; Solomon, E. I. *J. Am. Chem. Soc.* **1990**, *112*, 2243–2249.

(5) (a) Andréasson, L.-E.; Brändén, R.; Reinhammar, B. *Biochim. Biophys. Acta* **1976**, *438*, 370–379. (b) Andréasson, L.-E.; Reinhammar, B. *Biochim. Biophys. Acta* **1979**, *568*, 145–156. (c) Reinhammar, B. *Chem. Scr.* **1985**, *25*, 172–176.

(6) *Rhus vernificera* laccase was isolated[7] from the acetone powder (Saito and Co., Osaka, Japan) to a purity ratio A_{280}/A_{614} of 14.5–15.5, as modified in ref 8. The T1Hg derivative of laccase was prepared according to published procedures[9] as modified in ref 4 using a hollow fiber dialysis unit (Spectrum Medical Instruments, Los Angeles).

(7) Reinhammar, B. *Biochim. Biophys. Acta* **1970**, *205*, 35–47.

(8) Spira-Solomon, D. J.; Solomon, E. I. *J. Am. Chem. Soc.* **1987**, *109*, 6421–6432.

(9) Morie-Bebel, M. M.; Morris, M. C.; Menzie, J. L.; McMillin, D. R. *J. Am. Chem. Soc.* **1984**, *106*, 3677–3678.

0002-7863/91/1513-8544$02.50/0